Experiment M4: Photoluminescence

II. Institute of Physics A, RWTH Aachen

April 14, 2016

Contents

Contents

Required knowlege:

- Quantum mechanics of the interaction of light and matter, Fermi's golden rule, perturbation theory.

- Semiconductor band structure, doping

- Excitons

- Laser, 4-level-system

- Light diffraction by a grating

1 Introduction

In spectroscopy, frequency and intensity of emitted, absorbed or reflected radiation are analysed. By this, information about the interaction between radiation an matter, and their electronic structure are gained. Historically, spectroscopy was mainly confined to visible light which was emitted or absorbed by atoms and molecules. Nowadays, spectroscopy ranges over a wide range of frequencies and is used to gain insight in the electronic structure of a material (emission or absorption of photons), phonons in the solid state (Raman spectroscopy), crystal structure (X-Ray diffraction), core spins and structure of individual atoms or molecules (NMR), and many other material properties.

Luminescence describes the radiation emitted by a material which originates from the transition of the system from an excited state into the ground state. In the case of **Photo luminescence** the excitation is induced optically by the absorption of photons.
In photo luminescence spectroscopy, electrons are optically excited into a level far above the band edge. Subsequently, the electrons relax to the band minimum and emit luminescence radiation. The spectral composition of this light can give information about the sort of states at the band edge, transition probabilities or *e.g.* vacancies and impurities

2 Fundamentals

2.1 Quantum theory of the light - mater interaction

To describe the interaction between light and matter a semi classical approach is used. The electrons are treated quantum mechanically, while the light is described as an electromagnetic wave. To describe an electron in an electromagnetic field, the quantum mechanical momentum $\hat{p}$ in the unperturbed Hamiltonian has to be changed to $\hat{p} + e\hat{A}$ with the vector potential $\hat{A}$ of the field. This yields

$$\hat{H} = \frac{1}{2m_0}(\hat{p} + e\hat{A})^2 + V(r) \tag{1}$$

$$= \hat{H}_0 + \frac{e}{2m_0}(\hat{p} \cdot \hat{A} + \hat{A} \cdot \hat{p}) + \frac{e^2\hat{A}^2}{2m_0} \tag{2}$$

where $\hat{H}_0$ is the Hamiltonian of the unperturbed system. Using the Coulomb gauge, the products of the operators are interchangeable and can be merged. Neglecting the quadratic term in $\hat{A}$ one gets

$$\hat{H} = \hat{H}_0 + \hat{H}' \tag{3}$$

$$\text{with} \quad \hat{H}' = \frac{e}{m_0}\hat{p} \cdot \hat{A}. \tag{4}$$

If the eigenvalues E_m and eigenfunctions ψ_m of $\hat{H}_0$ are known, it is possible to calculate the effect of $\hat{H}'$ on the electronic states within the perturbation theory. To achieve this, one has to consider the time dependence of the coefficients a_m of the eigenstates ψ_m ($|a_m(t)|^2$ gives the probability, that an electron is in state ψ_m at the time t).

For an harmonic perturbation (plane, linearly polarised wave with frequency ω)

$$\hat{A}(r,t) = \hat{A}_0 e^{ikr} e^{-i\omega t} + \text{c. c.} \tag{5}$$

the result on a system in state ψ_m at time $t = 0$ is, in 1st order,

$$a_j^{(1)}(t) = -\frac{1}{\hbar}\frac{e^{i(\omega_{jm}-\omega)t} - 1}{\omega_{jm} - \omega}\hat{M}'_{jm} - \frac{1}{\hbar}\frac{e^{i(\omega_{jm}+\omega)t} - 1}{\omega_{jm} + \omega}\hat{M}'_{jm}, \tag{6}$$

with $\omega_{jm} = (E_j - E_m)/\hbar$ and $\hat{M}'_{jm}$ the matrix element

$$\hat{M}'_{jm} = \langle\psi_j|\,\hat{H}'\,|\psi_m\rangle = \int d^3 r \psi_j^* \hat{H}' \psi_m. \tag{7}$$

It is obvious, that transitions are only allowed for $\hbar\omega \approx (E_j - E_m)$ (conservation of energy).

An electromagnetic wave is able to induce a transition either from a lower to a higher level (absorption) or from a higher to a lower level (stimulated emission), as long as the origin state is occupied and the final state is unoccupied (*cf.* Fig. 1). The transition rate

$$W_{m \to j} = \frac{|a_j|^2}{t} = \frac{2\pi}{\hbar} \left| \hat{M}'_{jm} \right|^2 \delta(E_j - E_m - \hbar\omega) \tag{8}$$

describes the probability of a transition from state ψ_m to ψ_j per time ((**Fermi's golden rule**).

A more thorough discussion is found in most books about theoretical quantum mechanics. [1]
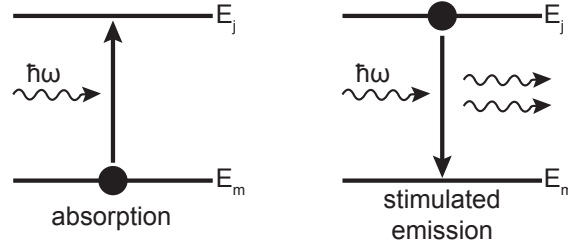

Figure 1: Optically induced absorption and emission between two discrete energy levels.

The opposite process of absorption, spontaneous emission, where excited electrons fall from a energetically higher onto a lower level without external influences, cannot be explained with this semi classical theory. To explain spontaneous emission, the electromagnetic field has to be quantised in the framework of a quantum field theory, which will not be discussed here. The time when the transition occurs is not predictable, only a probability and the lifetime of the excited state can be calculated.

2.2 Optical transitions in the solid states

In a solid state body, the discrete energy levels m,j turn into continuous energy bands. A number of different processes of light-matter interaction controls the optical properties of a solid. The model used here only describes inter band transitions through a band gap E_G. To achieve this, the delta function in Eq. (8) is replaced by a factor $g(\hbar\omega)$ which gives the combined density of states of the initial and final states, *joint density of states*, of the system.

The simple density of states (DOS) of an electron in a parabolic band is identical to the DOS of a free electron where the electron mass, m_e, is replaced by the effective mass m^*.

$$g(E) = \frac{1}{2\pi} \left(\frac{2m^*}{\hbar^2} \right)^{\frac{3}{2}} E^{\frac{1}{2}} \tag{9}$$

For the description of inter band transitions, the DOS of electrons and holes in parabolic bands are combined (see *e.g.* [2]) and it is,

$$g(\hbar\omega) = 0 \quad \text{for} \quad \hbar\omega < E_G \tag{10}$$

$$g(\hbar\omega) = \frac{1}{2\pi^2} \left(\frac{2\mu}{\hbar^2} \right)^{\frac{3}{2}} (\hbar\omega - E_G)^{\frac{1}{2}} \quad \text{for} \quad \hbar\omega > E_G \tag{11}$$

with the reduced electron-hole-mass

$$\frac{1}{\mu} = \frac{1}{m_e^*} + \frac{1}{m_h^*}. \tag{12}$$

In Addition to the combined DOS, the transition-matrix element $\hat{M}'_{jm}$ (*cf.* equation 8) is the leading factor. This will be shown, looking at an interband transition in a solid.
The e^{ikr}-term in eq. 5 is expanded into a Taylor expansion to

$$e^{ikr} = 1 + ik \cdot r + \frac{1}{2}(ik \cdot r)^2 + \dots . \tag{13}$$

For the interaction of electromagnetic waves with a wavelength in the order of visible light ($\lambda \approx 1\,\mu\text{m}$) with atoms whose diameters are in the order of $10^{-10}\,\text{m}$, only the first term has to be used as $|k \cdot r| \approx 10^{-3}$. This approximation is called the electrical dipol approximation.
The matrix element simplifies to

$$\hat{M}'_{jm} = \frac{2e}{m_0} \langle \psi_j | \hat{p} \cdot \hat{A}_0 | \psi_m \rangle . \tag{14}$$

The transitions of the outer valence band (vb) and the conduction bands (cb) in a solid are described by Bloch-waves

$$\psi_{vb,cb}(r) = \frac{1}{\sqrt{V}} \cdot u_{vb,cb}(r) \cdot e^{ik_{vb,cb} \cdot r}, \tag{15}$$

where $u_{vb,cb}(r)$ are lattice periodic functions.

By looking at a transition, induced by a photon with k_{opt} from the valence- to the conduction band and replacing the $\psi_{j,m}$ in equation (14) with Bloch-waves, it is shown that there is a contribution only for $k_{vb} = k_{cb} - k_{opt}$. As the wave vector of the electrons is some orders of magnitude larger that the momentum of the photon, one gets

$$k_{vb} \approx k_{cb}. \tag{16}$$

This shows, that the wave vector of the electron stays approximately constant and only 'straight' transitions in the $E(k)$ diagram are possible.

If an electric dipole transition is possible does not only depend on the energy and momentum of the respective states. A quantum mechanical consideration of dipol transitions of electrons within an hydrogen atom which is characterised with the quantum numbers n, l, m_l and m_s yields the following selection rules

- $\Delta m_l = 0, \pm 1$.

- $\Delta l = \pm 1$. The total momentum of electron and photon (± 1) is conserved.

- $\Delta m_s = 0$. Spin conservation.

These rules are also applicable to atoms with many electrons, or solids, where the electronic states are described by atomic wave functions.

In transitions which are forbidden by the selection rules, magnetic dipole or quadrupole transitions may occur which result from the higher order terms in eq. 13. The transitions have considerably lower transition probabilities and happen on a longer time scale (10^{-6} s). Slow emission due to these transitions is called **phosphorescence**. Emissions due to inter-band recombinations of electron-hole pairs happen on a much shorter time scale (10^{-9} to 10^{-8} s). This process is called **fluorescence**.

2.3 Optical transitions in semi conductors

Due to their band structure, semiconductors are separated in two sub categories. In a direct semiconductor (*e.g.* GaAs, GaN, ZnO) the maximum of the valence band (VB) and the minimum of the conduction band (CB) are "above one other" in momentum space with identikal $k = 0$. Optical transitions for valende band electrons into the conduction band are hence possible under eq. 16, as soon as the photon energy fulfils $\hbar\omega > E_G$.

Usually the CB minimum is not in the centre of the Brillouin zone, but at $k \neq 0$. Due to eq. 16, and as shown in Fig. 2, direct transitions are not possible. The difference in momentum between VB maximum and CB minimum have to be compensated by an additional emission or absorption of phonons. These are called **indirect semiconductors** (*e.g.* Si).

In real semiconductors a number of optical transitions occur at energies below
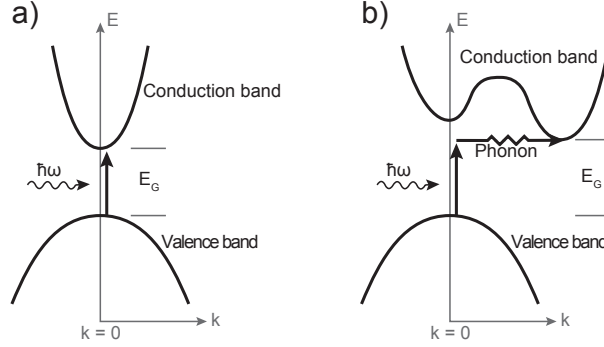
Figure 2: Transitions from valence to condution band in a a) direct and b) indirect semi conductor.

E_G. Possible reasons are e.g. doping or defects such as impurities, vacancies or interstitial atoms. These local disturbances yield discrete energy levels which usually reside just above the VB (*e.g.* acceptor levels) or below the CB (*e.g.* donor levels).

Another effect leading to a sharp absorption peak below the band edge in many materials is the excitation of exciton. This will be discussed in Section 2.6.

2.4 Photoluminescence

Photoluminescence is the process of emitting radiation by spontaneous recombination of an optically excited photon. This usually happens with photon energy $\hbar\omega > E_G$ where an electron-hole pair with momentum $\hbar k \neq 0$ is created (*cf.* Fig. 3). Due to strong electron phonon coupling, these 'hot' electrons relax, by emitting a photon, to the minimum of the CB. This process takes place on very fast times cales $\approx 100\,\text{fs}$. It can hence be assumed, that most electrons are completely relaxed prior to recombination via an inter band transition (order of 10^{-9} to $10^{-8}\,\text{s}$).

The same holds for holes, which relax to the VB maximum before recombining with an electron from the CB at $k = 0$.

2.5 Optical spin orientation and polarised photoluminescence

The photoluminescence of a sample can also be used to gain infromation about the spin properties of the excited electrons, see Fig. 10. The basic principles of this are the selection rules discussed in section 2.3 which couple the spin of the excited electrons to the polarisation of the photons. The optical excitation

Figure 3: Electrons (holes) which are excited by photons with an energy of $h\nu_L$ relax via phonon emission into the lowest (highest) unoccupied state in the conductionband (valenceband). The subsequent recombination under the emission of radiation is called photoluminescence. [2]
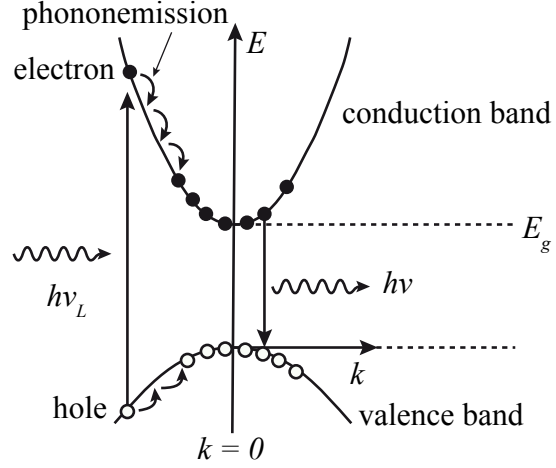
with circularily polarised light allows only transitions with an angular momentum transfer of $\Delta m = \pm 1$ as the total angular momentum is conserved. These are sketched on the left of Fig. 4 for right-handed circularly polarised light and on the example of GaAs. As the probabilities for the transitions $|-3/2\rangle \rightarrow |-1/2\rangle$ and $|-1/2\rangle \rightarrow |+1/2\rangle$ are different (3:1), the use of circularly polarised light yields a spin polarisation of the excited electrons in the CB.

$$P = \frac{n_\uparrow - n_\downarrow}{n_\uparrow + n_\downarrow} = \pm 50\%. \tag{17}$$

This is called optical spin orientation.

During the recombination of electrons and holes, the same selection rules apply and, depending on the transition, either right- or left-handed circularly polarised

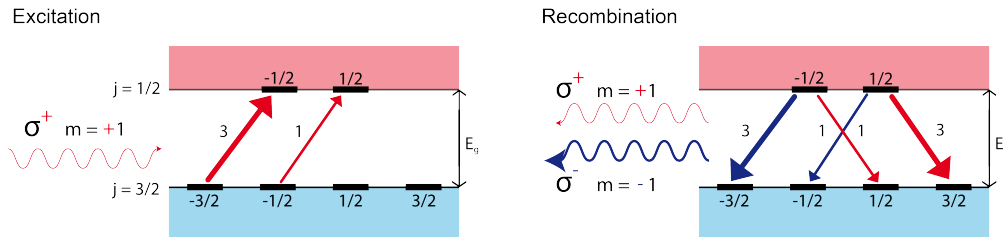**Figure 4:** Left: optical spin orientation using right-handed circularly polarised light in GaAs. Due to the selection rules, only the two sketched transitions are allowed, whose probabilities are 3:1. The resulting spin polarisation in the CB is 50%. Right: For the recombination, the same selection rules apply which results in a degree of polarisation of the circularly polarised light of 25%.

light is emitted. As before, the different probabilities have to be taken into account (*cf.* Fig. 4 right hand side) which yields a degree of polarisation of the PL light of

$$P_{circ} = \frac{I_+ - I_-}{I_+ + I_-} = \pm 25\% \tag{18}$$

after the excitation of an electron spin polarisation of 50% due to circularly polarised light. Generally the degree of polarisation of the PL-light can be attributed to the spin polarisation of excited CB electrons.

2.6 Excitons

Electrons and holes, which are generated by the absorption of photons, are spatially at the same place in the solid. Oppositely charged, they attract each other due to Coulomb interactions. This may yield bound, hydrogen-like states of the electron-hole pair which are called **exciton**.

Excitons are be split in two main categories: WANNIER-MOTT- and FRENKEL-excitons.

WANNIER-MOTT-excitons are weakly bound electron-hole pairs with a large radius which mainly occur in semiconductors. The binding energy is calculated in accordance with Bohr's model of the hydrogen atom. The high dielectric constant ϵ_r of the medium in which the exciton exists has to be taken into account. The reduced mass of the proton and electron $1/\mu = 1/m_e^* + 1/m_h^*$ are replaced by the effective mass of electron and hole in the solid. This yields:

$$E_n = -\frac{\mu}{m_e}\frac{1}{\epsilon_r^2}\frac{R_H}{n^2} = -\frac{R_X}{n^2} \tag{19}$$

with the Rydberg constant $R_H = 13{,}6\,\text{eV}$. The radius of the exciton is

$$r_n = \frac{m_e}{\mu}\epsilon_r n^2 a_B = n^2 a_X, \tag{20}$$

where a_B is the Bohr radius of the hydrogen atom.

Typical binding energies and radii are shown in Fig. 5. Note that WANNIER-MOTT-excitons stretch over many lattice constants. As they are able to move freely through the solid, these excitons are called free excitons.

FRENKEL-excitons on the other hand are strong bound and have small radii in the order of the lattice parameter. Due to their smaller size, the assumption of a homogeneous material is not valid any more and the surrounding of the ecition has to be taken into account as well. Hence, the model in eq. 19 cannot be used anymore to calculate the binding strength. Experimentally one gets values of a couple of $10\,\text{meV}$ up to $1\,\text{eV}$ in some organic semiconductors.

Bound excitons form when a free exciton binds to a defect or donor atom, ehereby it gains more energy.

For the optical properties of semiconductors excitoons play an important role, as they often dominate the absorption spectrum just below the band edge. Electrons are able to be excited into the CB although the photon energy is not sufficient, the missing energy is taken from the binding energy of the exciton.

In many materials, excitons are only observable at low temperatures as for the formation of stable excitons the binding energy needs to be higher than the thermal

Crystal	E_g (eV)	R_X (meV)	a_X (nm)
GaN	3.5	23	3.1
ZnSe	2.8	20	4.5
CdS	2.6	28	2.7
ZnTe	2.4	13	5.5
CdSe	1.8	15	5.4
CdTe	1.6	12	6.7
GaAs	1.5	4.2	13
InP	1.4	4.8	12
GaSb	0.8	2.0	23
InSb	0.2	(0.4)	(100)

Figure 5: Band gap E_g, excitonic Rydberg-constant R_X and exciton-Bohr-radius a_X of some semiconductors from [2].

energy of the phonons in the material.

2.7 Temperature dependence of the PL-peaks

The temperature dependence of the PL intensity of exciton peaks is explained by the equation for the rate equation for the exciton population.

$$\frac{dN_X}{dt} = G - (\gamma_r + \gamma_{nr})\, N_X. \tag{21}$$

Here, N_X is the number or density of the excitons in question and G the excitation rate thereof. γ_r and γ_{nr} are the rates for radiative (r) and non-radiative (nr) transitions. In equilibration $dN_X/dt = 0$ one gets the equilibrium population

$$N_X = \frac{G}{\gamma_r + \gamma_{nr}}. \tag{22}$$

The intensity of the PL-peaks is obviously given by the radiating transitions,

$$I(T) = \gamma_r \cdot N_x = \frac{\gamma_r}{\gamma_r + \gamma_{nr}} \cdot G. \tag{23}$$

The temperature dependence of the PL-intensity is in the transition rates γ_r and γ_{nr}. The non-radiative transitions describe transitions from one excitonic state into another and can be modelled by a Boltzman-factor,

$$\gamma_{nr} = \gamma_{nr}^0 \cdot e^{-\frac{\delta E}{k_B T}}, \tag{24}$$

while the radiative transitions, *e.g.* the recombination processes, which emit PL-light, can be approximated as independent of temperature,

$$\gamma_r = \gamma_r^0 = \text{const.} \tag{25}$$

δE is the energy difference between the initial and final excitonic state of the non-radiative transitions. Inserting this term in eq. 23, this yields the temperature dependence of the PL-intensity

$$I(T) = \frac{I_0}{1 + \gamma \cdot e^{-\frac{\delta E}{k_B T}}} \tag{26}$$

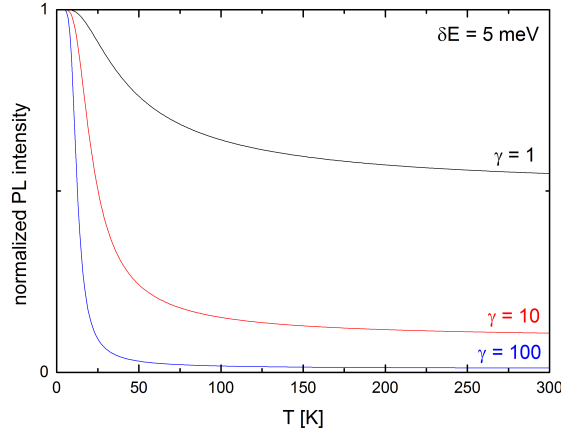with $\gamma = \frac{\gamma_{nr}^0}{\gamma_r^0}$. This function is simulated in Fig. 6 simuliert.

Figure 6: Temperature dependence of the PL-intensity for $\delta E = 5$ meV and for different values of γ.

For the case of $\gamma \cdot e^{-\frac{\delta E}{k_B T}} \gg 1$ (*i.e.* $\gamma \gg 1$ and $k_B T \geq \delta E$) the peak intensity is

$$I(T) \approx \frac{I_0}{\gamma} \cdot e^{+\frac{\delta E}{k_B T}}. \tag{27}$$

For high temperatures $k_B T \geq \delta E$ this yields an approximately exponential function of the peak intensity of the inverse tempreature $1/T$, as sketched in Fig. 7 as the non-radiative transitions dominate (if $\gamma \gg 1$).

In addition to the temperature dependent change in PL-intensity of the excitonic peaks, the peak position $E_{\text{peak}}(T)$ also changes with temperature. The change in position dependes on the temperature dependent change of the band gap, which
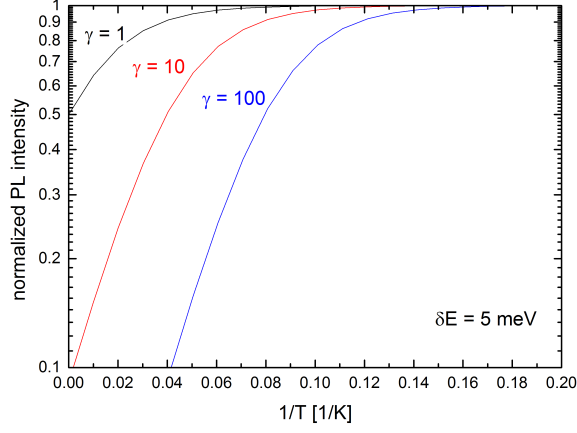
Figure 7: Temperature dependence of the PL-intensity for $\delta E = 5$ meV and for different values of γ. For high temperatures this is an almost exponential function of the intensity of inverse temperature $1/T$, as $\gamma \gg 1$.

is described by the phenomenological VARSHNI-formula [3]

$$E_g(T) = E_g(T = 0\text{K}) - \alpha\,\frac{T^2}{T + \beta}. \tag{28}$$

Herem α and β are meterial specific constants. For the exciton energies this yields $E_{\text{peak}}(T) = E_g(T) - E_b$ with the total binding energy of the excitons E_b. The latter resembles the binding energies of an electron and a hole of a free exciton, as well as additional contributions due to the localisation of the exciton at a defect site.

3 Sample system

3.1 Zinc oxide (ZnO)

Zinc oxide as a II-VI-semiconductor of great scientific interest (*cf.* [4] as an overview). Due to its large band gap of $E_G = 3{,}44\,\text{eV}$ it is ideal for opto-electronic devices in the near UV-range as *e.g.* blue LEDs.

The emission spectrum of ZnO is dominated by excitons, whose binding energy of 60 meV is well above the thermal energy at room temperature ($\approx 25\,\text{meV}$) and hence yields the possibility to use ZnO for Lasers or LEDs based on excitonic emission, which would have very narrow defined energies.

As ZnO is easily n-doped with *e.g.* Aluminum and is transparent to visible light, it is also ideal as transparent conducting layer (TCO, *transparent conducting oxide*). These are used in touch-screens or flat-screens or as a front electrode for solar cells, where the otherwise occurring shading is omitted.

line	wavelength (nm)	energy (eV)	localisation energy (meV)	two-electron-satellite separation ($2P_{xy} - 1S$) (meV)	donor binding energy (meV)	chemical identity
A_L^{*}	367.12	3.3772				
A_T^{*}	367.26	3.3759				
I_0	367.63	3.3725	3.4			
I_1	367.71	3.3718	4.1			
I_{1a}	368.13	3.3679	8.0			
I_2^{**}	368.19	3.3674	8.5			
I_3^{**}	368.29	3.3665	9.4			
I_{3a}	368.34	3.3660	9.9			
I_4	368.34	3.3628	13.1	34.1	46.1	H
I_5	368.86	3.3614	14.5			
I_6	368.92	3.3608	15.1	38.8	51.55	Al
I_{6a}	368.96	3.3604	15.5	40.4	53	
I_7	369.01	3.3600	15.9			
I_8	369.03	3.3598	16.1	42.1	54.6	Ga
I_{8a}	369.08	3.3593	16.6			
I_9	369.37	3.3567	19.2	50.6	63.2	In
I_{10}	369.76	3.3531	22.8	60.2	72.6	
I_{11}	370.28	3.3484	27.5			

[*] A_L and A_T are the longitudinal and transversal free A-exciton states. A_T is the reference for the determination of the bound exciton localisation energy.
[**] I_2 and I_3 are assigned to ionised donor bound exciton recombinations.

Figure 8: Classification of the excitonic emission peaks in ZnO [5].

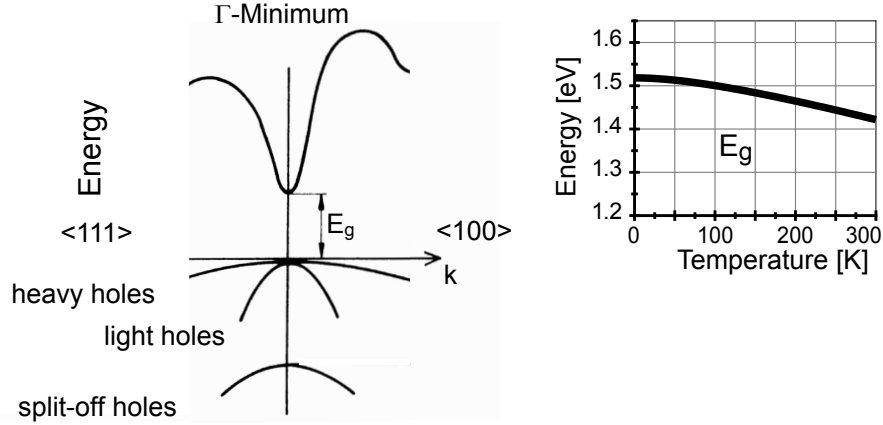The optical spectrum of ZnO is governed by free excitons at room temperature

Figure 9: Band structure of GaAs and the temperature dependence of the band gap energy.

and by a number of emission lines originating from bound excitons at low temperatures. Depending on the sample, up to eleven different lines are observable. These result mainly from excitons which are bound to neutral or ionised donor atoms. A thorough assessment and characterisation of the lines was done by Meyer *et al.*. [5] A summary of results is shon in the table in Fig. 8. The localisation energies of the bound excitons, which add to the binding energies of free excitons of $\approx 60\,\mathrm{meV}$, are in the order of a few meV. This explains why bound excitons are only stable at low temperatures.

Some of the lines are attributed to certain elements to which the excitons are bound. A PL-measurement on ZnO can hence give an insight in the used donor atoms.

The sample to be examined consists of a some hundred of nm thick *pulsed laser deposition* (PLD) grown thin film on a saphire substrate.

3.2 Gallium arsenide (GaAs)

Gallium arsenide is a III-V semiconductor with a direct bandgap of $E_g = 1{,}42$ eV at $T = 300$ K (*cf.* Fig. 9). The material is of high technological relevance. It is especially prominent for its long spin lifetimes of over 100 ns at low temperatures and ideal doping at the metal-insulator transition of $n(\mathrm{Si}) \approx 3 \cdot 10^{16}$ cm^{-3} in spin electronic. [6, 7].
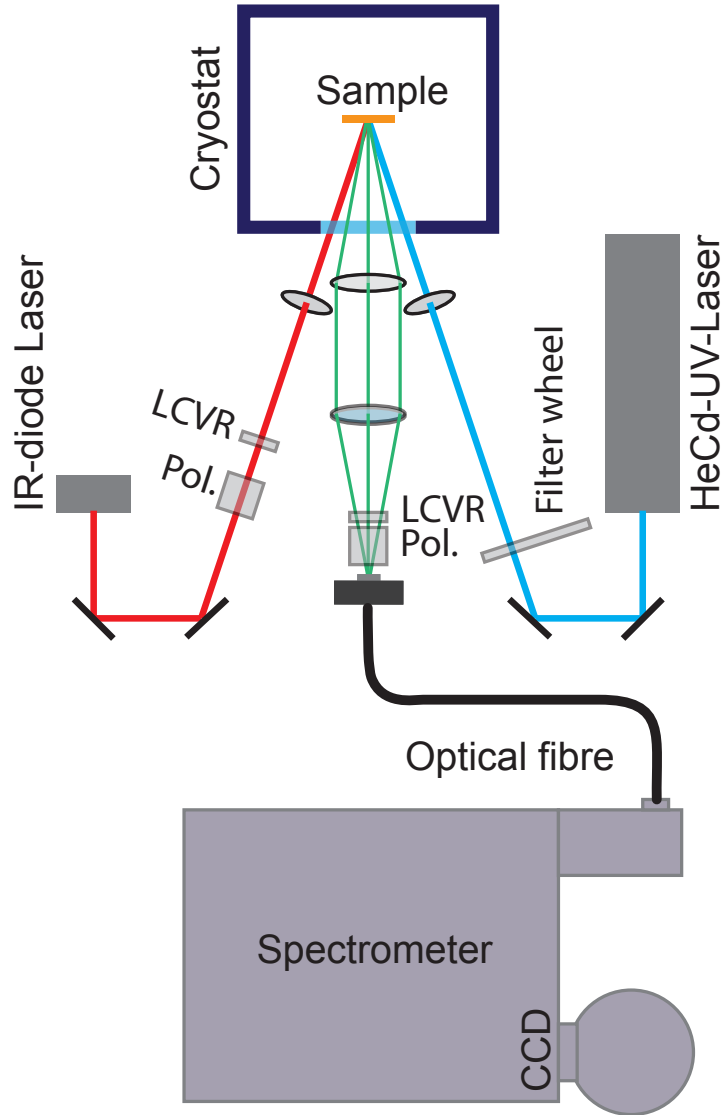
4 Experimental setup

Figure 10: Schematic of the experimental setup

The experimental setup is sketched in Fig. 10 and is briefly described hereafter. A Helium-Cadmium UV gas Laser is used for excitation of the ZnO sample and an IR diode laser for the examination of the GaAs sample. The laser light is focussed onto the sample using mirrors and lenses. For the excitation of a spin polarisation, a polariser and a liquid crystal variable retarder (LCVR) are placed inside the IR light path. This produced the circularly polarised light, necessary for the optical
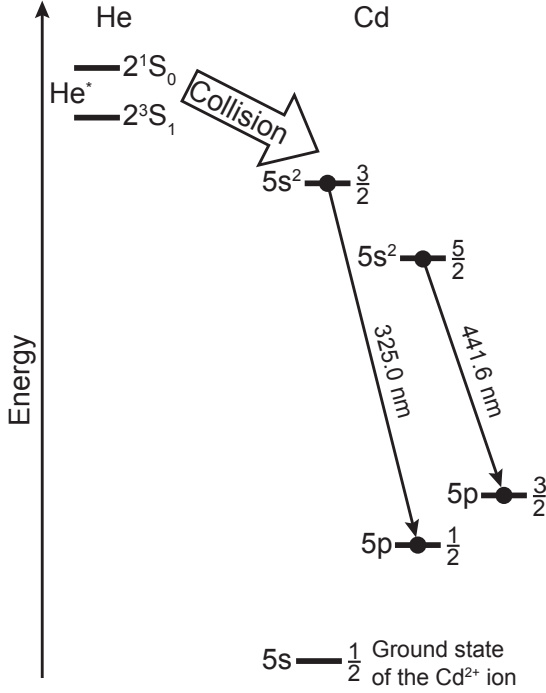
Figure 11: Energy states of Helium and Cadmium ions according to [8]. The 2^3S_1 and 2^1S_0 states of the excited Helium atom are higher in energy than the $5s^2$ states of the Cadmium ion. Due to collisions, the energy is transferred into the latter states.

spin orientation.

The samples are inside a cryostat and are optically accessible through a window. The cryostat is cooled with liquid Helium and allows to measure at temperatures between 4.2 K and 300 K. The temperature of the sample is controlled via cooling with liquid Helium and counter heating with a heater.

The emitted PL light is collected by a lens outside of the cryostat's window and parallelised. Another lens focuses the light into a glas fiber, which guides the light to the spectrometer. This is used to measure the spectral intensity distribution of the PL radiation.

To measure the degree of circular polarisation of the PL light after the optical excitation of a spin orientation in the GaAs, the right-handed and left-handed circularly polarised parts of the light are separated. Another LCVR is used to split the light into vertically and horizontally polarised light. By choosing the correct voltage of the LCVR, only one type of polarisation orientation is detected by the spectrometer. To measure the degree of polarisation, both orientations have to be measured.

Below, the basic principles of some of the components are discussed in more detail.

4.1 Laser

As excitation source for the measurements in the UV a HeCd gas laser is used. The active medium is a Helium and Cadmium metal vapour mixture. The He atoms are excited via gas discharge and give the energy to the Cd atoms via collisions. The Cd atoms are now ionised and excited. The radiative recombination produces the characteristic Laser line wavelengths. The dominant transitians are from the 5s to the 5p level (cf. Fig. 11) which belong to emission lines at $\lambda = 325$ nm and $\lambda = 442$ nm. The Laser used here emitts the energetically higher wavelength of 325 nm.

For the polarisation dependent measurements on GaAs a GaAs/GaAlAs diode laser is used. This emits light between 808.4 nm and 812.9 nm. The power is controlled by limiting the current on the controller. The exact principles of a laser can be found in the instructions for the lab-course "Nd-YAG-Laser".

4.2 Spectrometer

A spectrometer is used to measure the energy and intensity distribution of the measured radiation. In optical spectrometers, the light is spatially split up by a dispersion element such as a prism or a grating.

In this experiment a grating is used as shown in Fig. 12. The light enters through a slit shaped entrance aperture of variable width and shines onto a collimation mirror. The mirror is used to parallelise the light, so that the grating is evenly illuminated. As a reflection grating is used, light of different wavelengths is reflected in different directions. Another difractive mirror focuses the light onto the detector where different wavelengths are detected at different positions on the detector.

4.2.1 Diffraction grating

To explain the principle of a diffraction grating, one usually considers the principles of multiple slits first. The overlap of the spherical waves from the individual slits leads to constructive and destructive interference depnedning on wavelength and observation direction. The main maxima of nth order occur at

$$n \cdot \lambda = d \cdot \sin(\beta_n) \tag{29}$$

(gratings equation) in an angle β_n measured against the face normal of the grating. $d = \frac{1}{m}$ is the grating parameter and m the density of slits which is often used to characterise the grating.

A high number N of light slits leads to narrower and more defined main maxima, between which an increasing number $(N - 2)$ of sub-maxima are (see Fig. 13).

The spectral resolution $\frac{\lambda}{\Delta \lambda}$ gives the value for the difference in wavelengths around
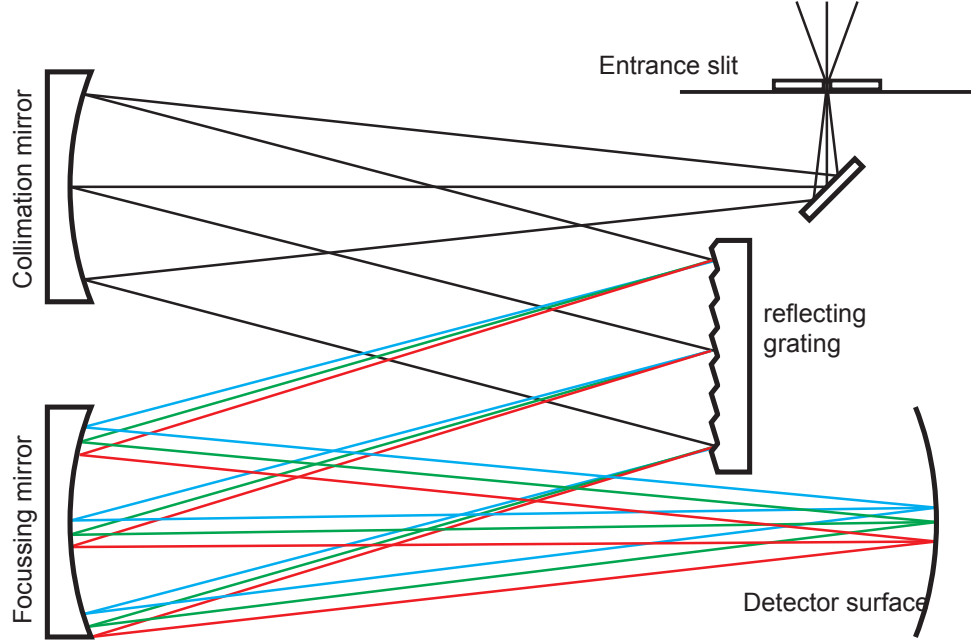
Figure 12: Schematics of the used spectrometer (Czerny-Turner-configuration)

one main wavelength λ for two lines to be able to be separeted. For optical gratings it is

$$\frac{\lambda}{\Delta\lambda} = nN. \tag{30}$$

In the experiment a reflection instead of a transmission grating is used as sketched in Fig. 14 (b). In the most simple case, these are just a number of grooves in the material. However, usually one uses a saw-tooth profile to gain better results. By tuning the angle of the saw-tooth, a high intensity for a certain wavelength and a vertain order is achieved. This is called a *blazed grating*.

The grating equation is corrected for the reflective grating to

$$n \cdot \lambda = d \left(\sin(\beta_n) - \sin(\alpha) \right). \tag{31}$$

Reflection gratings have the advantage, that no intensity is lost via absorption at the bars of the grating.

4.2.2 CCD

To record the light intensity as a function of wavelength, a *charge-coupled device* (CCD) is used. CCDs are one- or two-dimensional sensors which are commonly used in digital cameras. Fro their invention, W. Boyle and G. E. Smith won the

Figure 13: Intensity distribution after a diffraction grating on (a) 2, (b) 4 and (c) 8 slits, from [9].
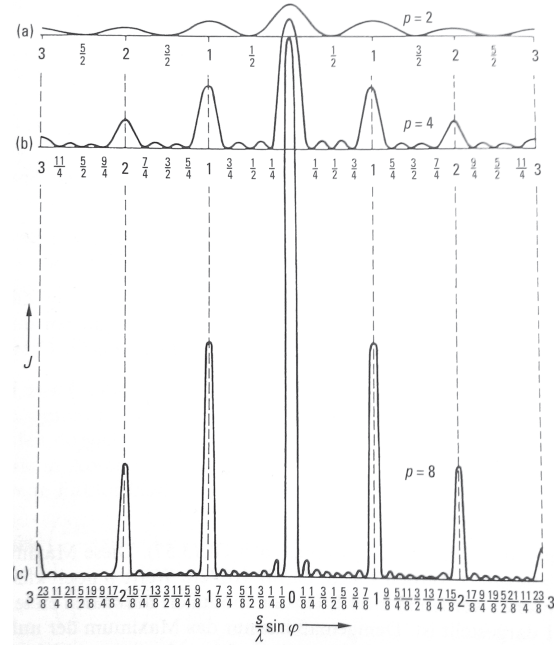
Figure 14: Diffraction caused by a grating. The diffraction pattern is caused by the overlay of spherical waves originating from individual steps. Due to the different positions of the steps, these have a difference in optical path. Left: *specular* reflection at the 'virtual' surface of the grating (gray), diffraction of 0th order. Right: Diffraction maxima for different wavelengths in the 1st order reflection.
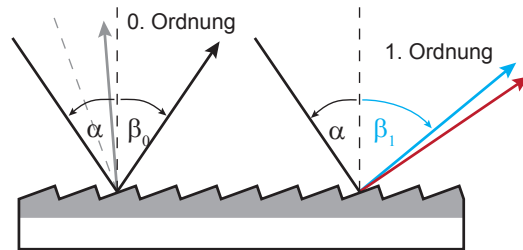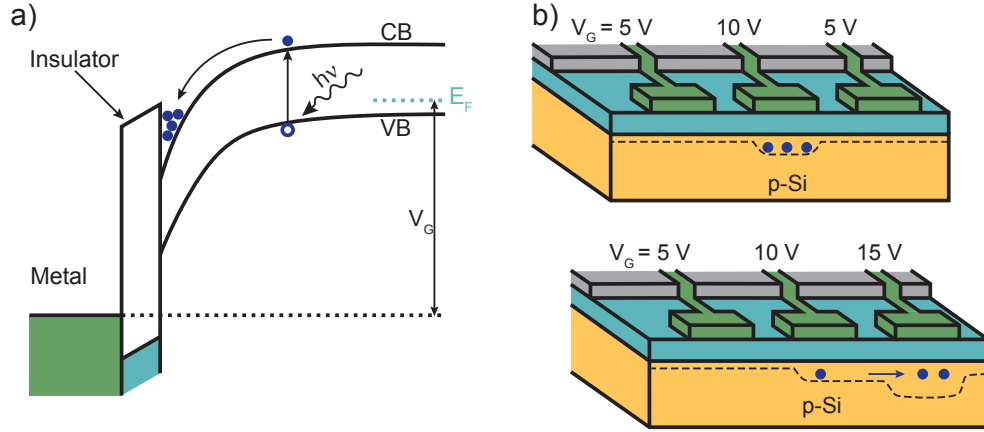
Figure 15: *Charge-coupled Device.* a) Bandstructure of a MOS-Diode, b) schematics of a CCD-sensor [10].

2009 Nobel price.

CCD sensors are based on a stack of a doped semiconductor, an insulator and a transparent electrode on top. At the boundary between semiconductor and insulator, due to band bending, a potential well is formed in the conduction band of the semiconductor (*cf.* Fig. 15 (a)). If hit by light of a certain wavelength, electron-hole pairs are formed. Along the semiconductor-insulator interface a conductive channel forms. Using different gate potentials as shown in Fig. 15 (b), potential wells are formed where the accumulated charges are stored. The accumulated charge is proportional to the amount of light shone onto the device.

For the read-out, the charge in neighbouring cells is stepwise changed and the electron packets are shifted to the next cell.

The sensor used in this experiment is made from a one dimensional CCD chain with 1380 pixels. To reduce thermal noise, the sensor is cooled with liquid nitrogen during the measurement.

5 Conducting the experiment and tasks

At the beginning of the day of the experiment the CCD-chip of the spectrometer should be cooled with liquid nitrogen under supervision of the tutor. During the oral exam, the temperature can begin to settle. Also the Laser should be switched on to allow for stabilisation of the working temperature.

5.1 Working with Lasers: Safety instructions

The radiation emitted by the Lasers has a power of a couple 10 mW. Already much lower power can irreparably damage the eyes! Always wear Laser safety glasses when the Lasers are switched on. This protects you from accidentally reflected radiation during adjustment of the light path. However, the glasses only partially block the radiation. Even with glasse on:

<div align="center">
Never look directly into the Laser beam!
Never lower your head down to the hight of the Laser beam!
</div>

While working on the Laser beam remove all watches, rings, bracelets and other reflective objects which might cause reflections. Be careful that the metallic Allen keys or the optical holders never come into the light path. Always block the Laser with a white card (or, in case of the UV Laser, the shutter) when adjusting the optics.
All optics cause back reflections. Take extra care that all reflections hit the black shields around the setup and are not able to hit any metallic surface.

5.2 Adjustment of the Laser beam

The Laser beam should be aligned by the tutor in a way that they hit the sample under the same angle and thus be reflected back in the same light path. This results in a similar adjustment of the two beams. You should nevertheless control the alignment using the markings on the table and the calibration iris. To do so, adjust the Laser to a power of 1 mW and check for the correct hight of the beam and that all optics (such as mirrors, lenses and polarisers) are hit centrally. To achieve the back reflection in the same path, the cryostat, and hence the samples, might have to be rotated.

If using the Laser power meter the following rules apply:

- The λ-key is used to set the wavelength for which you wish to adjust the power. Confirm with "OK".

- The arrow keys change the range "R".

We recommend to start with the ZnO measurements using the UV-Laser as the PL-light of ZnO is slightly blueish and visible to the eye. That eases the alignment of the detection optics. To align the detection optics, you probably have to remove the safety glasses as these also shield the visible light. You should only do so if you are sure that the Laser beam is carefully adjusted and no metallic object can be hit be the beam. After finishing the adjustment you should use the safety glasses again. Now hold the white card behind the collimation lens and move it towards the collimation lens for the fibre. Adjust the fibre in a way that it is centrally hit by the focused PL-light. A fine adjustment can be made by optimising the peak heights of the recorded spectra.

If swapping the Laser to IR, only very small adjustments to the fibre should be necessary to optimise the signal of the PL-spectra.

5.3 Recording of PL-spectra: Spectrometer Software

CCD and spectrometer are controlled and read-out by the software *Syner JY V3.5* which is build into *Origin*. The software records spectra by measuring the CCD counts per chosen time interval. You can change the settings in the menu

Collect → Experiment Setup.

The spectrometer has two different gratings with different parameters (lines/mm). The coarse grating has 120 lines/mm and a lower spectral resolution, but a wider spectral field which is recorded compared to the fine grating with 1200 lines/mm. The latter has the better spectral resolution, but is only able to record a range of about 40 nm. However, for recording a high resolution spectrum, the fine grating can still be used, as the software is able to stitch the spectra together. The grating is chosen at

Monos → Grating.

The measuring range can be set in one of two ways: Either by choosing a central wavelength (*Detectors → CCD Position*) or by choosing a start and end wavelength (*Detectors → CCD Range*). In the latter case, a number of spectra are recorded and stitched together if the range is larger than the range of a single spectrum. Make sure that the Laser wavelength is not in the set range, as the high intensity of the Laser might damage the CCD of the spectrometer.

For the correct recording of PL-spectra the exposure time of the CCD sensor has to be set via

Detectors → Exposure Time.

After the change of experimental parameters such as Laser power, alignment or sample temperature, the exposure time has to be set to the lowest value (0.01 s) to avoid damage to the CCD sensor. The maximum signal the sensor can record

are 60000 counts. If necessary change the exposure time (up to a factor of 10) to use the maximum amount of counts and optimise the signal-noise ratio. However, for all new settings, a background measurement should be recorded, where the Laser is blocked. This background can than be subtracted from the measured data. Make sure that *Detectors → Dark Substract* is switched off, as this would subtract another, not fitting dark measurement which does not correspond to your actual measurement.

The software also allows the record of multiple spectra in a row and to average these. (*Detectors → Accumulations* resp. *Detectors → Cycles*) Recording a sequence of measurements might be usefull during the fibre adjustment. If you do not want to use that function, set all values to '1'.
The recorded spectra are presented as a graph and an Origin worksheet. You can either work with the worksheets in Origin, or save these for another application.

5.4 Temperature dependent measurements on ZnO

5.4.1 Measurements

Investigate the temperature dependence of bound excitons in the existing ZnO sample. You should record PL-spectra between 10 k and 100 K in suitable temperature steps. Choose an appropriate range of wavelengths and set the exposure time accordingly. After changing parameters, remember to record an additional noise measurement with identical settings for subtraction. For once, also record one spectrum which shows the Laser wavelength with an exposure time of 0.01 s. This is to verify the calibration of the spectrometer.

5.4.2 Analysis of the measurements

Identify the individual exciton peaks of ZnO. Which impurities can be identified? Analyse the temperature dependence of the peaks (peak height, width and position) and determine the localisation energies of the excitons.

5.5 Polarisation measurements on GaAs

5.5.1 Conducting the measurements

Set the sample temperature to 10 K. Change to the GaAs sample by aligning the cryostat horizontally and vertically so that the IR Laser beam hits the sample. Check the alignment of the fibre via maximising the peak heights in the PL spectra. To do so, record a couple of spectra without polarising optics (Polariser and LCVR).

After fine adjustment of the fibre, you have to set the voltage of LCVR where linearly polarised light is transformed to circularly poilarised light and *vice versa*. To set the LCVR voltage the driver with two LCVRs must be connected to the computer over USB and the program "LC Driver" must be started. The voltages driving both LCVRs can be set independently from each other. A $\lambda/4$ retardation can be achieved at voltages $U_{\sigma+} = 1.97$ V and $U_{\sigma-} = 4.07$ V. Place both polarisers in the incoming beam and adjust their optical axes to be parallel by measuring the Laser power behind the polarisers. When are the optical axes parallel? After that, place the second polariser and one of the LCVRs between the focussing lens and the fibre in the detector area. Take care for the correct orientation with respect to the beam direction.

Measure the degree of polarisation of the PL-light at 10 K. Remember to take a noise measurement.

5.5.2 Analysis

Identify the visible peaks in the circularly polarised light I_+ and I_- by a literature research. Analyse and discuss the spectrum for the degree of circularly polarisation of the PL-light according to eq. 18. Does this measurement show what you expected?

5.6 Tips and tricks for analysing spectra

This section deals with some problems which might occur by analysing the spectra and how to avoid these.

As shown in table 8 many excitonic transitions can lay very close together in the PL-spectra and even overlap. Figure 16 shows a simulation of four overlapping peaks with a constant background. The individual peaks are shown in green, red, blue and orange, while the total signal is shown in black. The first three peaks are so close together, that their signal has to be described as the sum of the peaks. It is obvious, that in this case, the peak amplitudes cannot be read straight from the maxima in the total spectrum. While for peak 2the error is acceptable, the amplitude for peak 1 and 3 would be highly exaggerated. Peak 4 on the other hand has a distance to the other peaks wich is large enough to read the amplitude from the maximum of the spectrum at that position. A direct extraction of the peak amplitudes and widths is only justified if the peaks do not overlap.

In the case of overlapping peaks, a multi-peak fit has to be used. (Individual single-peak fits do not yield the correct results, as these will not take the contributions of neighbouring peaks into account. Single peak fits are only justified
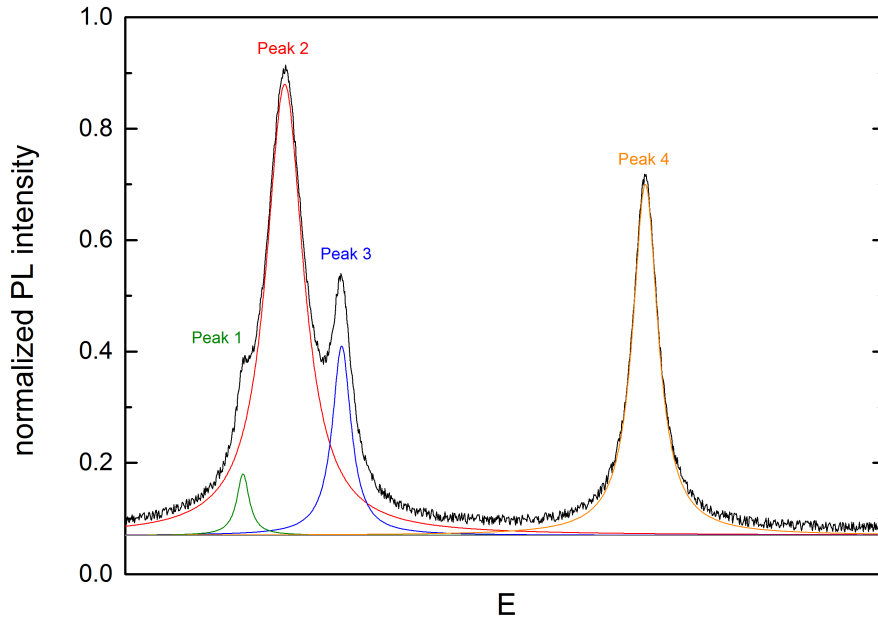
Figure 16: Simulation of four overlapping LORENTZ-Peaks and a constant background. A meaningful analysis of peaks 1 - 3 is only possible via a multi-peak fit.

if the peak is separated.) Multi-line fits can be done using *Origin* which can be used in the CIP-Pool of the Physikzentrum or via remote desktop connections to the Rechenzentrum. A brief description follows. Of course, you can use any other software as well.

Usually the individual exciton peaks can be approximated by LORENTZ-peaks of the shape

$$I(E) = \frac{I_0}{1 + \left(\frac{E - E_{\text{peak}}}{\Delta E/2}\right)^2},$$

(32)

as is usual for resonances of dipole oscillations. I_0 is the peak amplitude, E_{peak} the peak position and ΔE the full width at half maximum (FWHM). (In the case of phonon contributions to the exciton transitions, GAUSS-peaks can also occur. This, however, is not relevant in the course of this course.) In *Origin* you fin dthe fit function for individual or overlapping LORENTZ-peaks at

Analyse → Anpassen → Nichtlinearer Fit → Dialog öffnen.

Under

Einstellungen → Funktionsauswahl in *Kategorie: Origin Basic Functions*
you find *Funktion: Lorentz*. Using the taps you can have a look at the equation
(*Formel*) of the function and at a plot (*Beispielkurve*) of the function.
At *Einstellungen → Erweitert → Kopien* you can change the number of copies.
If fitting a single peak set this to '0'. For *e.g.* three peaks, set it to '2' copies.
In the tab *Parameter* the initial values for the peaks are set. Change these if the
automatically set values seem to be unreasonable. The fit function, using the set
initial values, is shown in the tab *Fit-Kurve* together with the chosen measured
data. Here you can control the quality of the initial parameters.
At *Einstellungen → Erweitert → Fit-Steuerung* the maximum number of iteration
Max. Anzahl der Iterationen can be changed. This might be useful if the chosen
starting parameters do not lead to a convergent fit with the pre-set number of
iterations.
There are a number of additional settings, although the above mentioned are the
most important settings and should yield meaningful fit results.
Important: When analysing a series of measurements, make sure to normalise the
PL-spectra to laser power and exposure time, so that the peak heights can be
compared with each other.

5.7 Remarks about the report

The report should include the aim of the experiment as well as a detailed descrip-
tion of the procedure of the experiment. The main part of the protocol contains
the presentation and the analysis of the data. You should show an overview of
the measured spectra and discuss the in the frame of the analysis described in the
Sections 5.4 and 5.5.

6 Questions for self-control

- What is FERMI's golden rule?

- What is the thermal energy at room temperature?

- Which order of magnitude have the binding energies of free excitons? At which temperatures can these be observed?

- What is the difference between WANNIER-MOTT- and FRENKEL-excitons?

- Why can the binding energy of a FRENKEL-Exzitonen not be calculated in analogy to the Hydrogen atom?

- What are the differences between interband transitions and transitions with exciton contributions in the PL-spectrum?

- Which orientation of the retarder with respect to the polariser is necessary to measure only left-handed or right-handed circularly polarised light of the PL-light?

- How can you show, mathematically, that the degree of polarisation of the PL-light after optical spin orientation reaches ideally 25%?

- Which influence has a n-doping of the GaAs sample on the degree of polarisation of the PL-light?

- How does the number of lit slits of a diffraction grating influence the intensity distribution?

- Which properties should a diffraction grating have to reach the highest resolution?

- What is the advantage of a reflection grating compared to a transmission grating? What is the advantage of the saw-tooth geometry of the grating?

- How does a CCD sensor work? What happens if the exposure time is too long, or the light intensity too high?

References

[1] H. Kurz, Vorlesungsskript Optoelektronik I.2.

[2] M. Fox, *Optical Properties of Solids* (Oxford University Press, 2001).

References

[3] I. Vurgaftman, J. R. Meyer, und L. R. Ram-Mohan, J. Appl. Phys. **89**, 5815 (2001).

[4] C. Klingshirn, M. Grundmann, A. Hoffmann, B. Meyer, und A. Waag, Physik Journal **5**, 33 (2006).

[5] B. K. Meyer *et al.*, Phys. Status Solidi B **241**, 231 (2004).

[6] J. M. Kikkawa und D. D. Awschalom, Phys. Rev. Lett. **80**, 4313 (1998).

[7] R. I. Dzhioev *et al.*, Phys. Rev. B **66**, 245204 (2002).

[8] C. S. Willett, *Introduction to gas lasers: population inversion mechanisms* (Pergamon Press Ltd., 1974).

[9] L. Bergmann und C. Schaefer, *Lehrbuch der Experimentalphysik Band 3, Optik, Wellen- und Teilchenoptik* (Walter de Gruyter & Co., 2004).

[10] S. M. Sze, *Physics of Semiconductor Devices* (John Wiley & Sons, Inc., 1981).